Rapid and Simultaneous Determination of Montelukast, Fexofenadine and Cetirizine Using Partial Least Squares and Artificial Neural Networks Modeling

Hassaninejad-Darzi, Seyed Karim*[+]

Department of Chemistry, Faculty of Sciences, Babol Noshirvani University of Tehnology, Babol, I.R. IRAN

Es'haghi, Zarin; Nikou, Seyed Mohammad

Department of Chemistry, Faculty of Sciences, Payame Noor University, Tehran, I.R. IRAN

Torkamanzadeh, Mohammad

Department of Chemistry, Faculty of Science, Babol Noshirvani University of Tehnology, Babol, I.R. IRAN

ABSTRACT: *Simultaneous determination of pharmaceutical compounds and accurate quantitative prediction of them are of great interest in the clinical and laboratory-based investigations. This work has focused on a comprehensive comparison of Partial Least-Squares (PLS-1) and Artificial Neural Networks (ANN) as two powerful types of chemometric methods. For this purpose, montelukast (MONT), fexofenadine (FEXO) and cetirizine (CET) were studied as three pharmaceuticals whose UV-Vis absorption spectra highly overlap each other. The cross-validation leave-one-sample-out procedure was applied and the optimum number of factors was determined. The developed models were subsequently validated through testing with an independent dataset. Furthermore, a simple and fast method for wavelength selection (WS-PLS-1) in the calibration step was presented which involved the calculation of the Net Analyte Signal Regression Plot (NASRP) for each test sample. Highest prediction accuracies corresponded to WS-PLS-1 method with R^2 values of 0.994, 0.982 and 0.999 for MONT, FEXO and CET, respectively. The best values of detection limit was also provided by WS-PLS-1 method which obtained to be 0.029, 0.049 and 0.054 mg/L for MONT, FEXO and CET, respectively. According to the results obtained, WS-PLS-1 method was shown to have the potential to be utilized as a promising tool in clinical and pharmaceutical applications.*

KEYWORDS: *Artificial neural networks; Partial least squares; Montelukast, Fexofenadine; Cetirizine; UV-Vis.*

***** *To whom correspondence should be addressed.*
+ E-mail: hassaninejad@nit.ac.ir
1021-9986/2017/3/81-96 *16/$/6.60*

INTRODUCTION

There are three main pharmaceuticals that their discovery has had a significant impact on treatment strategies for the management of asthma: Montelukast (MONT), Fexofenadine (FEXO) and Cetirizine (CET). MONT is a potent and selective antagonist of the cysteinyl leukotriene receptor which is utilized for the treatment of asthma [1]. FEXO is a non-cardiotoxic and non-sedative terfenadine metabolite, which acts as a selective second-generation histamine H_1 receptor antagonist, relieving the uncomfortable manifestations of rhinitis [2]. CET is a piperazine derivative and metabolite of hydroxyzine and is described as a long-acting non-sedating antihistamine with some mast-cell stabilizing activity.

One of the main difficulties in accurate determination of pharmaceuticals in clinical and laboratory applications is the fact that drug components are usually in mixtures rather than being single. The conventional spectrophotometric methods use a separate number of wavelengths that are not frequently enough to offer the necessary information to resolve a system with severe spectra overlapping [3]. Multivariate methods, however, allow extracting analytical information and permit a rapid analytical response with minimum sample preparation, reasonable accuracy and precision without separation procedures.

Among different regression methods commonly used for multivariate calibration, the factor analysis-based methods such as Partial Least Squares (PLS) have received considerable attention in the literature [4-6]. PLS offers a full-spectrum method and, therefore, efficient outlier detection methods are available from spectral residuals and chemically interpretable spectral information can be extracted from PLS analysis. This advantage allows for a rapid determination of mixture components often with no need of prior separation or sample pre-treatment [7]. PLS is a developed generalization of the Multiple Linear Regression (MLR). However, the ability to analyze highly collinear and noisy data is an advantage of PLS over MLR. MLR-based methods have the disadvantage that all significant components must be known, whereas the robust multivariate method of PLS can be calibrated by ignoring the concentrations of all other components except the analyte of interest (also known as leave-one-out procedure) [8]. An excellent review of the multivariate statistical method has been presented by *Martens & Naes* [9].

PLS can also be coupled with other evolutionary mechanisms such as Genetic Algorithm (GA) for chemometric analysis of data and optimization of the procedure parameters. For instance, *Khoshayand et al.* [10] exploited GA for the wavelength selection in PLS calibration without loss of prediction capacity in simultaneous determination of paracetamol, ibuprofen and caffeine in pharmaceuticals. GAs are widely applied to solve extremely complex problems with objective functions that do not possess 'nice' properties such as continuity, differentiability, etc [10, 11]. A number of typical samples and discussions on genetic algorithms can be found elsewhere [12-14].

The PLS method differs from Principal Component Regression (PCR) in including the dependent (concentration) variable in the data compression and decomposition operations. In other words, both concentration and spectra data are actively used in the data analysis. Because PLS and PCR models require information only about a single species, they can be significantly easier to implement [8, 15].

Aside from multivariate analysis method, Artificial Neural Networks (ANN) can also be utilized in order to differentiate between the complex absorption spectra resulting from the mixture of components. A number of layers, each having some neurons, with the aid of weights and biases make the network flexible for solving nonlinear complex problems and handling complicated systems [16, 17]. Recently, there has been a growing interest among researchers in applying neural networks to simultaneous determination of different analytes in biological, pharmaceutical and agricultural samples [18-20]. *Ni et al.* [21], for example, used ANN method in simultaneous spectrophotometric determination of three pesticides in vegetable and fruit samples. *Li et al.* [22] tried the ANN method to solve the problem of simultaneous determination of components of similar character, namely, the mixture of fluorescent dyes. Their results also indicated that ANN was a much more feasible strategy compared to PCR and PLS.

In respect of literature survey, no published method was reported for the simultaneously quantifying MONT, FEXO and CET that does not require a prior physical separation. This paper therefore aims to apply partial least squares technique and neural network modeling as two low-cost and rapid methods for simultaneous determination of these drugs by UV-Vis spectroscopy.

EXPERIMENTAL SECTION

Materials

Sodium montelukast (MONT), fexofenadine hydrochloride (FEXO) and cetirizine dihydrochloride (CET) were purchased from Sigma-Aldrich and methanol was prepared from Fluka Company. Stock standard solutions of MONT, FEXO and CET were prepared separately by dissolving 10 mg of each compound in 10 mL of methanol. The concentrations of each drug were 1000 mg/L (ppm) which would equal to 1.64×10^{-3}, 1.86×10^{-3} and 2.17×10^{-3} mol L^{-1} of MONT, FEXO and CET, respectively. Fig. 1 displays the molecular structures of these drugs.

Apparatus and software

Recording of the absorption spectra were performed using a UV-Vis spectrophotometer (LABOMED Instrument, double beam– Model UVD-3200). All measurements were carried out at 22 ˚C using a quartz cuvette of 1.0 cm optical path. Partial Least Squares-1 (PLS-1) and neural network modellings were implemented by MATLAB R2013a software (MathWorks). The MVC1 program featuring PLS-1 was written by *Olivieri et al.* [23].

Procedures

One component calibration

In order to find the Linear Dynamic Range (LDR) for each drug, different volumes of stock solution of each component was added to 25 mL volumetric flask and diluted to the mark with methanol. The electronic absorption spectra of all drugs were recorded over the range of 195–400 nm. Absorption values were recorded at the wavelength of 211, 205 and 204 nm with different concentration of the MONT, FEXO and CET, respectively. The LDR for each compound was achieved by plotting absorbance values versus drug concentration. The LDRs were obtained to be 1.0–35.0, 1.0–28.0 and 1.0–25.0 mg/L for MONT, FEXO and CET, respectively.

Calibration and test sets

By convenient dilution of the stock solutions, a calibration set of 36 samples, including binary- and ternary-component mixtures was built. Concentrations of the drugs used for the calibration set were in the range of 2.0–12.0 mg/L. Standard solutions were prepared in 25 mL volumetric flasks by addition of suitable amounts of each stock solution and diluted by methanol to the mark. Similarly, 15 additional samples were prepared to serve as the test set. The UV-Vis spectra of the corresponding solutions were recorded in the same spectral conditions at ambient temperature and the obtained data were used for PLS-1 and ANN modeling.

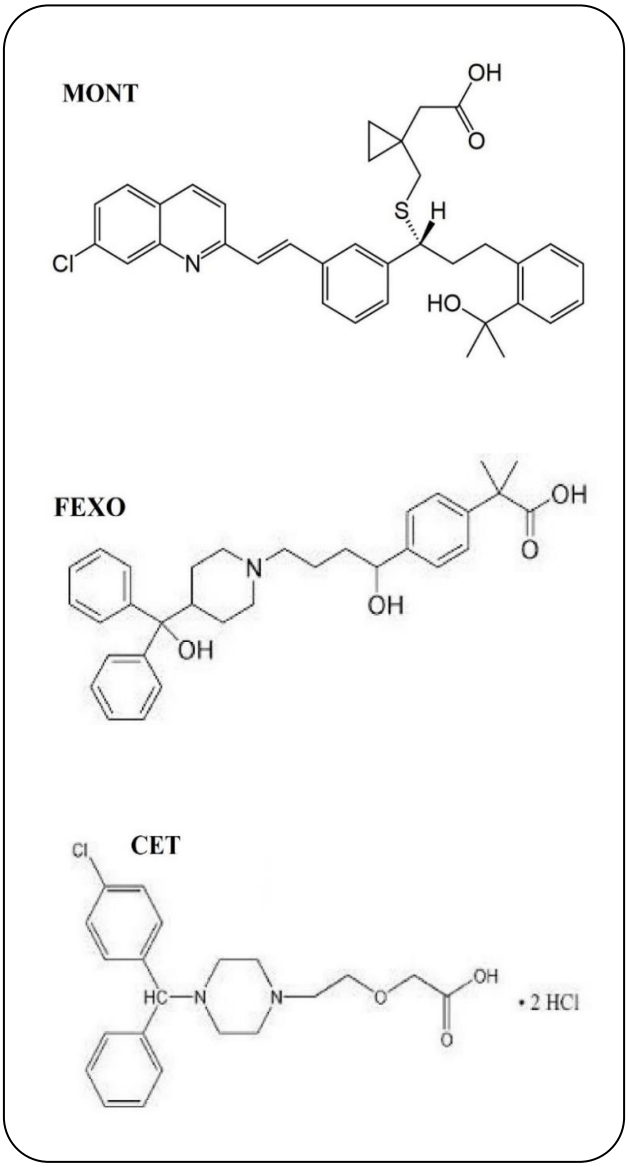

Fig. 1: Molecular structure of montelukast (MONT), fexofenadine (FEXO) and cetirizine (CET)

PLS modeling

PLS is factor-based chemometric method which can analyze highly collinear, noisy data. PLS is commonly

applied to the simultaneous analysis of two datasets such as spectra and concentration. Based on a number of factors (latent variables), PLS builds a linear model such as y=Xb which allows the prediction of concentration (*y*) from measured spectra (*X*), where *b* contains the regression coefficients that are obtained during the calibration step [24, 25]. To be more specific, *X* is the $n \times m$ matrix of measured responses obtained from spectrophotometry, with *n* equal to the number of samples and *m* equal to the number of sensors (analytical wavelengths). *y* is the $n \times c$ concentration matrix of *c* analytes. *b* is the $n \times c$ vector of regression coefficients which is solved for when PLS is calibrated [26]. With *b* in hand, the calibrated model can then predict new unknown *y* concentrations from measured *X* spectra.

ANN modeling

In this study, a MultiLayer Perceptron (MLP) feedforward network was applied for modeling the concentrations of MONT, FEXO and CET. As schematically shown in Fig. 2, the MLP consists of three types of layers: an input layer, an output layer and a hidden layer, each layer contains a number of neurons which operate in parallel. These neurons are connected by weights that are modified during the learning phase [27]. Implementing ANN model normally requires a number of steps: data collection, data pre-processing, building the network, training, testing, validation and data post-processing, successively. The whole procedure is summarized in the flowchart shown by Fig. 3.

Data collection

As a first step to designing an ANN model, the sample data is to be collected and prepared. In the present work, absorption measurement data of mixtures of MONT, FEXO and CET in the spectral range of 195-300 nm (106 points) were collected and fed to the system as model inputs. The concentration of the three above-mentioned component in the samples were the target (measured) outputs of the network.

Data pre-processing

It is believed that neural network training can be made more efficient if certain pre-processing steps are performed on the raw input and target data. Randomizing and normalizing data are the most common practices of

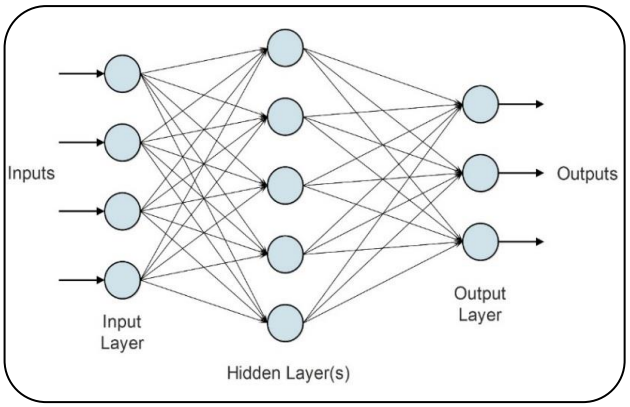

Fig. 2: Schematic representation of multi-layer feed-forward neural network architecture.

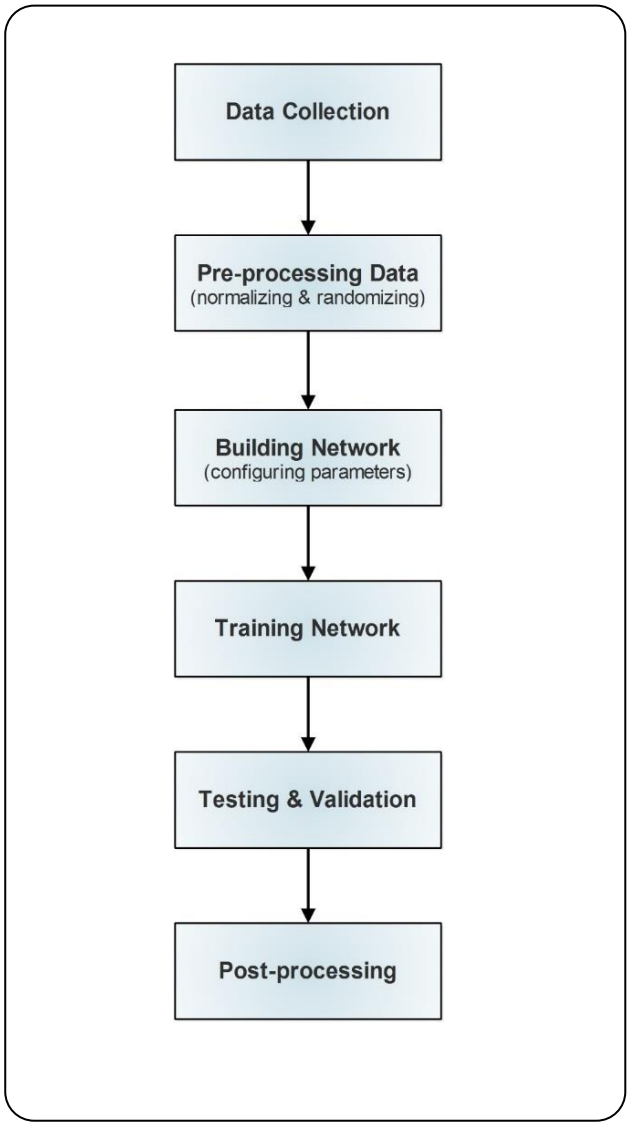

Fig. 3: Basic flowchart for designing artificial neural network model.

data pre-processing. Normalization procedure often makes the model more efficient as it prevents the learning algorithm from being confused by the unequal magnitude of different variables and consequently neglecting the variable with the smaller magnitude [28]. The data were scaled between -1 to 1 using the MATLAB function 'mapminmax'. The used equation is as follows:

$$\hat{x} = 2\left(\frac{x - x_{min}}{x_{max} - x_{min}}\right) - 1 \qquad (1)$$

where x_{min} and x_{max} are the minimum and maximum values of the unscaled dataset, xis the input value and $\hat{x}$ is the scaled input value. Other stages pertaining to the design of ANN model, including training and testing procedures, will be discussed subsequently in this paper.

RESULTS AND DISCUSSIONS

Spectral characteristics

Fig. 4 shows electronic absorption spectra of MONT, FEXO and CET. As can be seen, the spectrum of each drug is highly overlapped with the others. Therefore, these compounds cannot be determined in the presence of each other by a uni-variate calibration procedure unless with previous separation. The multivariate calibration method can instead be applied for determination of each drug in the mixtures. All spectra were recorded in the region between 195 and 300 nm with 1.0 nm steps (106 points per spectrum). The same method was performed for samples in the test and unknown sets.

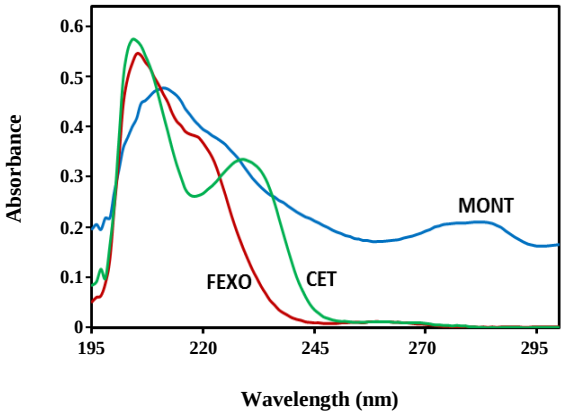

Fig. 4: Electronic absorbance spectra of MONT, FEXO and CET with a total concentration of 6 ppm (2 ppm each) in methanol.

PLS-1 method

Calibration and validation

In the first step to developing the PLS-1 model, a calibration set was built with a dataset of 36 samples, including binary- and ternary-component mixtures in order to take into account the different concentration ratios of analytes and to cover the range usually present in pharmaceutical samples. The combinations of concentrations of MONT, FEXO and CET in the calibration set is listed in Table 1.

The full cross validation method suggested by *Haaland & Thomas* [29] was used for the accurate selection of the optimum number of factors. This consisted of removing one sample at a time from the calibration step and carrying out the calibration by the remaining samples. The concentration of the one sample removed is expected with the achieved model. This step was repeated for each considered sample. The procedure can be repeated after fixing a different number of factors. Prediction Residual Error Sum of Squares (PRESS) was obtained from Eq. (2) and the best number of factors was selected in the minimum of PRESS values. In this equation, *m* is the number of samples in the calibration set and $C_{i,act}$ and $C_{i,pred}$ are the actual and predicted concentration of analyte in the ith sample, respectively [30].

$$PRESS = \sum_{i=1}^{m}\left(C_{i,act} - C_{i,pred}\right)^2 \qquad (2)$$

Similarly, the Standard Error of Cross-Validation (SECV) can also be defined as:

$$SECV = \left[\frac{\sum_{i=1}^{m}\left(C_{i,act} - C_{i,pred}\right)^2}{m}\right]^{1/2} \qquad (3)$$

In order to determine the optimum number of factors, SECV was plotted as a function of different number of factors, as shown by Fig. 5. As observed in this figure, high cross-validation errors is observed in small numbers of factors. This error is significantly reduced by increasing the number of factors. The optimum number of factors was found to be 3 for MONT, 5 for FEXO and 8 for CET at which SECV attained the least possible value. Afterwards, the developed PLS-1 model was applied to an independent test set including 15 artificial samples which were not used during calibration. The experimental

Table 1: Concentration of MONT, FEXO and CET in the calibration set. Concentration values are expressed as mg/L.

Sample no.	MONT	FEXO	CET	Sample no.	MONT	FEXO	CET
Ternary mixtures				19	11	11	11
1	12	12	12	20	11	11	3
2	12	12	2	21	3	11	11
3	2	12	12	22	3	3	11
4	12	2	12	23	11	3	3
5	2	2	12	24	3	3	3
6	12	2	2	25	7	7	3
7	2	12	2	26	7	11	7
8	7	7	7	27	11	7	7
9	7	7	2	28	7	3	7
10	7	12	7	Binary mixtures			
11	12	7	7	29	4	4	-
12	2	7	7	30	5	5	-
13	7	2	7	31	6	6	-
14	7	7	12	32	10	10	-
15	6	5	7	33	7	-	6
16	8	7	9	34	7	-	7
17	10	9	11	35	11	-	8
18	9	11	10	36	-	11	11

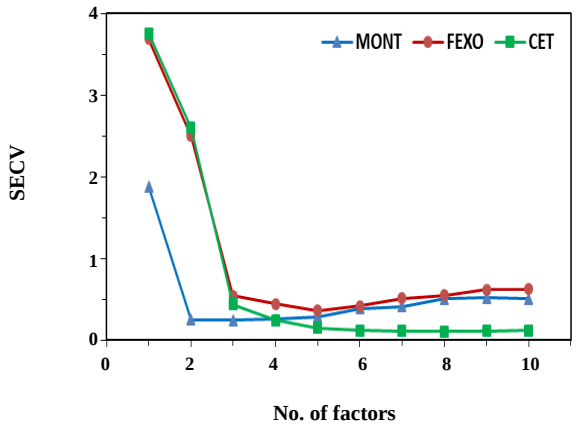

Fig. 5: Standard Error of Cross-Validation (SECV) vs. the number of factors in PLS regression.

and predicted concentration of each analyte can be seen in Table 2.

Analytical figures of merit

Figures of Merit (FOM) determination is obviously an essential part in the validation of chemometric methods. Toward this end, FOM such as selectivity (SEL), sensitivity (SEN), analytical sensitivity (γ) and Limit of Detection (LOD) may be defined and applied to compare the analytical methods used in the present study. The Net Analyte Signal (NAS) for Analyte k (r_k^*) is defined as the part of the signal that is orthogonal to the signal of the interferences present in the sample [15]. Ranging from 0 to 1, SEL is a measure of how unique the spectrum of the analyte is compared with the other species. It requires

Table 2: Composition of test set and predicted values for MONT, FEXO and CET by PLS-1, WS-PLS-1 and ANN regression. Concentration values are expressed as mg/L.

MONT				FEXO				CET			
Actual	PLS-1	WS-PLS-1	ANN	Actual	PLS-1	WS-PLS-1	ANN	Actual	PLS-1	WS-PLS-1	ANN
8.00	7.78	7.95	8.24	8.00	8.00	7.98	7.46	0.00	-0.14	-0.11	-0.23
9.00	8.79	9.01	9.47	9.00	9.04	9.08	8.81	0.00	-0.04	-0.02	0.35
3.00	3.38	3.22	2.60	0.00	0.30	-0.15	1.05	4.00	4.02	3.70	3.98
4.00	4.15	4.02	3.48	0.00	0.26	-0.17	0.41	5.00	5.15	4.86	4.92
12.00	12.12	12.03	11.90	0.00	-0.24	-0.05	-0.42	10.00	10.13	10.06	9.94
0.00	0.04	0.01	0.25	12.00	11.62	11.52	11.77	12.00	12.00	11.93	11.61
0.00	0.02	-0.02	0.32	10.00	9.50	9.64	9.99	10.00	10.07	10.03	10.16
4.00	4.01	3.97	3.76	6.00	6.01	6.09	5.92	5.00	5.17	5.06	4.27
5.00	5.35	5.32	5.40	4.00	3.90	3.88	3.59	6.00	5.99	6.06	5.90
11.00	10.22	10.08	10.91	3.00	2.30	2.46	3.16	11.00	10.67	10.75	11.04
3.00	2.87	3.00	2.85	11.00	9.96	10.16	10.76	3.00	2.85	2.93	2.79
7.00	6.95	6.91	7.37	7.00	5.83	6.18	6.23	7.00	6.70	6.86	7.25
3.00	3.16	3.13	2.71	7.00	5.73	6.02	6.31	7.00	6.87	6.79	7.05
7.00	7.10	6.91	7.56	7.00	6.02	6.18	6.78	11.00	10.97	11.05	11.37
2.00	2.39	2.35	1.55	2.00	2.78	2.42	3.09	2.00	2.38	2.11	2.47

that the part of the total signal that is not lost due to spectral overlap, and can be defined in the multivariate context by resorting to NAS calculation [31]:

$$\mathrm{SEL}=\frac{\left\|s_k^*\right\|}{\left\|s_k\right\|} \tag{4}$$

where || || means the Euclidian norm of vector, s_k is a spectrum containing analyte k at unit concentration and s_k^* is its corresponding NAS [32]. The sensitivity determines the variations in the response as a function of the concentration of a particular analyte [31], and is stated by the following equation:

$$\mathrm{SEN}=\left\|s_k^*\right\| \tag{5}$$

The analytical sensitivity (γ), which is defined in analogy with univariate calibration, is the ratio between SEN and the instrumental noise (ε), according to Eq. (6):

$$\gamma=\frac{\mathrm{SEN}}{\|\varepsilon\|} \tag{6}$$

where $||\varepsilon||$ is the amount of the instrumental noise. The value of $||\varepsilon||$ may be estimated from the standard deviation in the NAS of several blanks. Concerning the limit of detection, the following simple equation has been proposed for its estimation [33]:

$$\mathrm{LOD}=\frac{3\|\varepsilon\|}{\left\|s_k^*\right\|} \tag{7}$$

In order to enhance both the predictive ability and sensitivity of the PLS-1 method, the wavelength selection approach was applied. The algorithm searches for the minimum error indicator (EI) as a function of a moving window, starting from the Net Analyte Signal Regression Plot (NASRP) for each sample [34, 35]. According to *Skibsted et al.* [36], it is generally expected that the non-related spectral variation is rather large in pharmaceutical spectroscopic applications and thus it is important to be removed. Towards this end, a region of most informative wavelength (sensors) has been selected to minimize non-modelled interferences. The optimum wavelength range was determined to be 264-300 nm for MONT, 217-260 nm for FEXO and 222-255 nm CET.

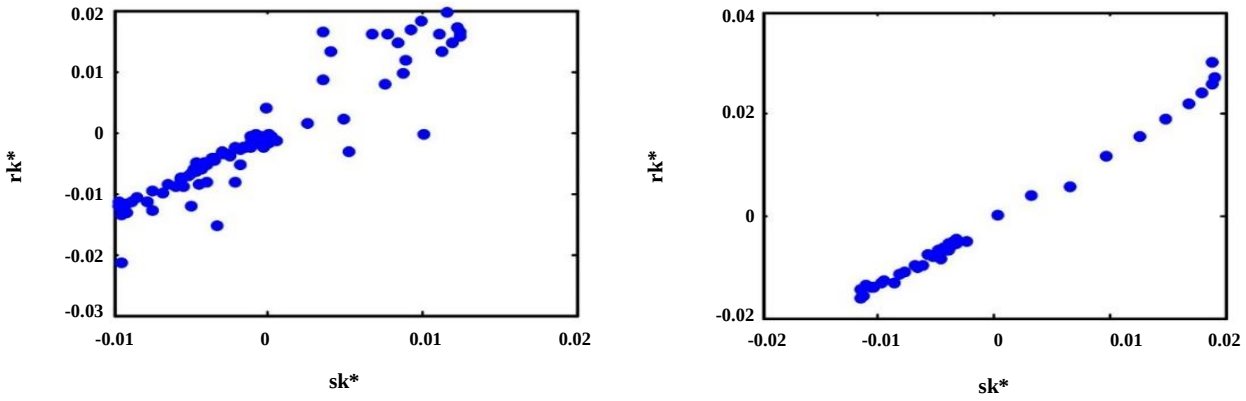

Fig. 6: Left panel: NASRP corresponding to FEXO using the calibration wavelength range 195-300 nm. Right panel: NASRP in the restricted sensor range of 217-260 nm

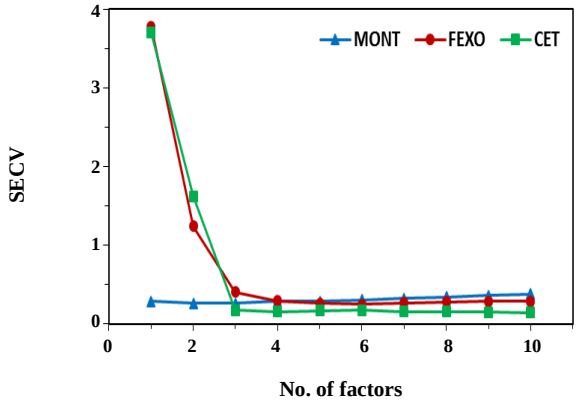

Fig. 7: Standard Error of Cross-Validation (SECV) vs. the number of factors in WS-PLS-1 regression.

As a typical example, an independent sample which was not used to make the calibration model was tested by the PLS-1 method. Fig. 6 shows the NASRP plots for the mentioned sample before and after applying wavelength selection methodology for FEXO. Fig. 6 (left panel) illustrates the NASRP for FEXO in the full spectral region of 195–300 nm. As observed, the data is highly distributed and linearity is not achieved, implying the presence of interferences which were not modeled during calibration. On the other hand, Fig. 6 (right panel) indicates that linearity is satisfactorily fulfilled in the restricted region of 217-260 nm, as suggested by the NASRP criterion.

Similar to PLS-1 method, the optimum number of factors in WS-PLS-1 can also be determined by plotting SECV vs. the number of factors, as shown by Fig. 7. By moving from one factor to three, a drastic decline in validation error is realized for FEXO and CET, whereas the variation of that for MONT is moderate. It can be concluded that SECV of different components sooner converges to its minimum in WS-PLS-1 method comparing to PLS-1 method (see Fig. 5).

In order to compare the prediction performance of the proposed WS-PLS-1 method with the earlier PLS-1 method, the developed WS-PLS-1 model was further simulated independently by a dataset of 15 samples. Table 2 lists the experimental and estimated content of MONT, FEXO and CET in these samples obtained by both methods. Comparing PLS-1 and WS-PLS-1, the agreement between the predicted data and the experimental results is higher regarding WS-PLS-1 method. It should be noted that the negative values seen in this table are actually denoting the zero amount of corresponding component (concentration) estimated by the model.

Comparison of PLS and WS-PLS performances

Table 3 shows several estimated FOM for MONT, FEXO and CET by PLS-1 and WS-PLS-1 models. According to Marsili et al. [15], analytical sensitivity is a measure which enables one to compare different analytical methods regardless of the specific technique, equipment, and scale employed. As observed by Table 3, the analytical sensitivity (γ) provided by WS- PLS-1 was enhanced considerably for all three drugs compared to the former PLS-1 method. In respect of selectivities, the highest value corresponded to MONT which was achieved by PLS-1 method. In contrast, FEXO showed the highest selectivity among other components in WS-PLS-1 method.

Table 3: Analytical figures of merit of the spectrophotometric method by applying PLS-1 and WS-PLS-1 regressions for MONT, FEXO and CET.

	PLS-1			WS-PLS-1		
Parameters	MONT	FEXO	CET	MONT	FEXO	CET
No. of Factors	3	5	8	3	3	3
SEN (AU*. L/mg)	0.25	0.06	0.04	0.05	0.06	0.05
SEL	0.60	0.31	0.26	0.26	0.56	0.42
γ (L/mg)	23	16	15	104	61	55
LOD (mg/L)	0.128	0.185	0.203	0.029	0.049	0.054

** AU is absorbance unit*

Table 4: Comparison of LOD (mg/L) with WS-PLS-1 regression described in this work with previously published works.

	Limit of detection (mg/L)									
	This work	Reported in literature								
MONT	0.029	0.293 [37]	0.1 [38]	0.009 [48]	0.003 [49]	0.01 [50]	0.2 [39]	0.094 [40]	0.0052 [51]	0.075 [41]
FEXO	0.049	3.007 [37]	0.01 [52]	0.0125 [53]	0.12 [42]	0.001 [54]	0.976 [43]	0.006 [55]	0.95 [44]	0.27 [45]
CET	0.054	0.037 [56]	0.10 [57]	0.02 [58]	0.379 [46]	0.0025 [59]	0.027 [60]	6.00 [47]	0.10 [45]	-

As can be seen in Table 3, while WS-PLS-1 method used less factors than PLS-1, it has improved LOD values almost four-fold. It can also be understood that the best LOD was obtained for MONT by both analytical methods. In order to challenge the detection performance of the proposed method, the LOD provided by WS-PLS-1 in this work was compared with a number of studies which have been previously published regarding the determination of MONT, FEXO and CET. As shown in Table 4, the LOD offered by the present study for all three drugs is clearly below the average of those reported by other works which studied the determination of MONT [37-41], FEXO [37, 42-45], and CET [46, 47] indicating a very good LOD which was provided via WS-PLS-1 method after selecting the appropriate wavelength range.

ANN method

In the second part of this work, the spectral data of each drug was used to develop a neural network model. For this purpose, the network parameters were specified. Among these parameters are; the number of hidden layer(s), number of neurons in each layer, transfer functions, training algorithm, performance function. In this study, one hidden layer with different number of neurons was tested with hyperbolic tangent sigmoid ('tansig') and Logistic sigmoid ('logsig') transfer functions. It was found that hyperbolic tangent sigmoid function provided the best fits to the data.

In order to train the network, the absorption spectra of a set of 36 calibration data shown by Table 1 (the same as previously used by PLS-1 and WS-PLS-1 methods) was used as model inputs. Concentrations of the three pharmaceutical components in each sample was considered as model targets. Matlab function 'mse' was utilized in order to measures the network's performance according to the mean-squared-errors (Eq. 8) and the network was trained using Levenberg-Marquardt ('trainlm') back-propagation training algorithm.

$$MSE = \frac{1}{n}\sum_{i=1}^{n}\left(C_{i,pred} - C_{i,act}\right)^2 \quad (8)$$

In order to determine the optimum number of neurons in the hidden layer, a series of calibration was performed through several runs, in which the number of neurons was varied from 1 to 10. Each topology was run repeatedly to avoid random correlation due to the random initialization

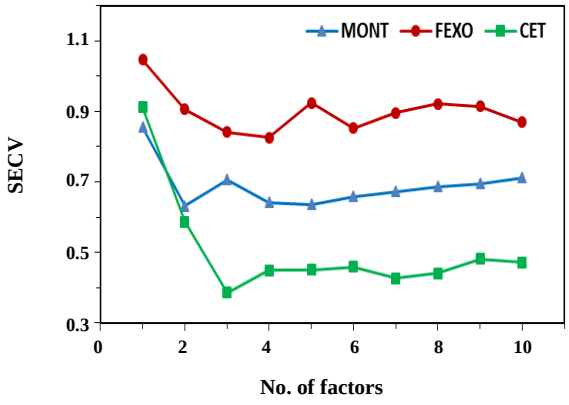

Fig. 8: Standard Error of Cross-Validation (SECV) vs. the number of neurons in the hidden layer.

of the weights [22]. The standard error of prediction committed by the cross-validation of the calibration set of each topology was calculated. As observed in Fig. 8, the optimum number of neurons in the hidden layer was found to be 2, 4 and 3 in the calibration of MONT, CET and FEXO, respectively.

The developed model which was trained in the previous stage was further simulated by a test set of 15 unknown data. The results obtained by ANN method is listed in Table 2 together with those predicted by the other methods investigated in this work and will be discussed subsequently.

Comparison of the predictive abilities of proposed methods

Once the optimal number of factors has been determined, the final calibration may be performed using all the calibration samples with the optimal number of factors (or neurons). As mentioned earlier, a set of independent test dataset of 15 samples which has not been used previously for calibration, was modeled by PLS-1, WS-PLS-1 and ANN methods. The predicted values of each component together with reference values can be seen in Table 2. Also, a residual analysis may be carried out by plotting absolute residual vs. the concentration of each analyte. Towards this end, the absolute residual was defined as the difference between actual concentration and the predicted value from a model. Fig. 9 demonstrates the residual values for the three drugs obtained by PLS-1, WS-PLS-1 and ANN models. As can be realized in these set of figures, the residual errors committed by WS-PLS-1 method are closely distributed around the zero-error line for all three components. Highest accuracies were obtained for prediction of CET with PLS-1 and WS-PLS-1 methods with all estimated concentrations close to the reference values. Prediction of FEXO seems to exhibit more deviations than the other components, however, this deviation between experimental and predicted values was mitigated by WS-PLS-1 method in comparison to the other regression models. In respect of MONT, model predictions are observed to be equally satisfactory given by each method.

Table 5 shows a number of important statistical parameters such as the determination coefficient of prediction ($R^2_{pred,}$ Eq. 9), root mean square error of prediction (RMSEP, Eq. 10) and relative error of prediction (REP, Eq. 11).

$$R^2_{pred} = 1 - \frac{\sum_{i=1}^{n}\left(C_{i,act} - C_{i,pred}\right)^2}{\sum_{i=1}^{n}\left(C_{i,act} - \bar{C}\right)^2} \quad (9)$$

$$RMSEP = \left[\frac{\sum_{i=1}^{n}\left(C_{i,act} - C_{i,pred}\right)^2}{n}\right]^{1/2} \quad (10)$$

$$REP\% = 100 \times \left[\frac{\sum_{i=1}^{n}\left(C_{i,act} - C_{i,pred}\right)^2}{\sum_{i=1}^{n}\left(C_{i,act}\right)^2}\right]^{1/2} \quad (11)$$

where $C_{i,act}$ and $C_{i,pred}$ is the actual and predicted concentration of a component in the i th sample, respectively. $\bar{C}$ is the mean of actual concentrations in a particular set and n is the number of samples in the test set.

This table also shows the values of the optimal number of factors and neurons used for both PLS-1 methods and ANN in the calibration set. As can be seen Table 5, the predictive ability of PLS-1 method was clearly improved after selecting the optimum region of sensors. The results also indicate that predictions of PLS-1 and WS-PLS-1 models for CET are in excellent agreement with experimental data, as high R^2 values of 0.998 and 0.999 was obtained for these methods, respectively. WS-PLS-1 also gave a lower RMSEP in all cases than PLS-1 and ANN methods. Looking carefully at Table 5,

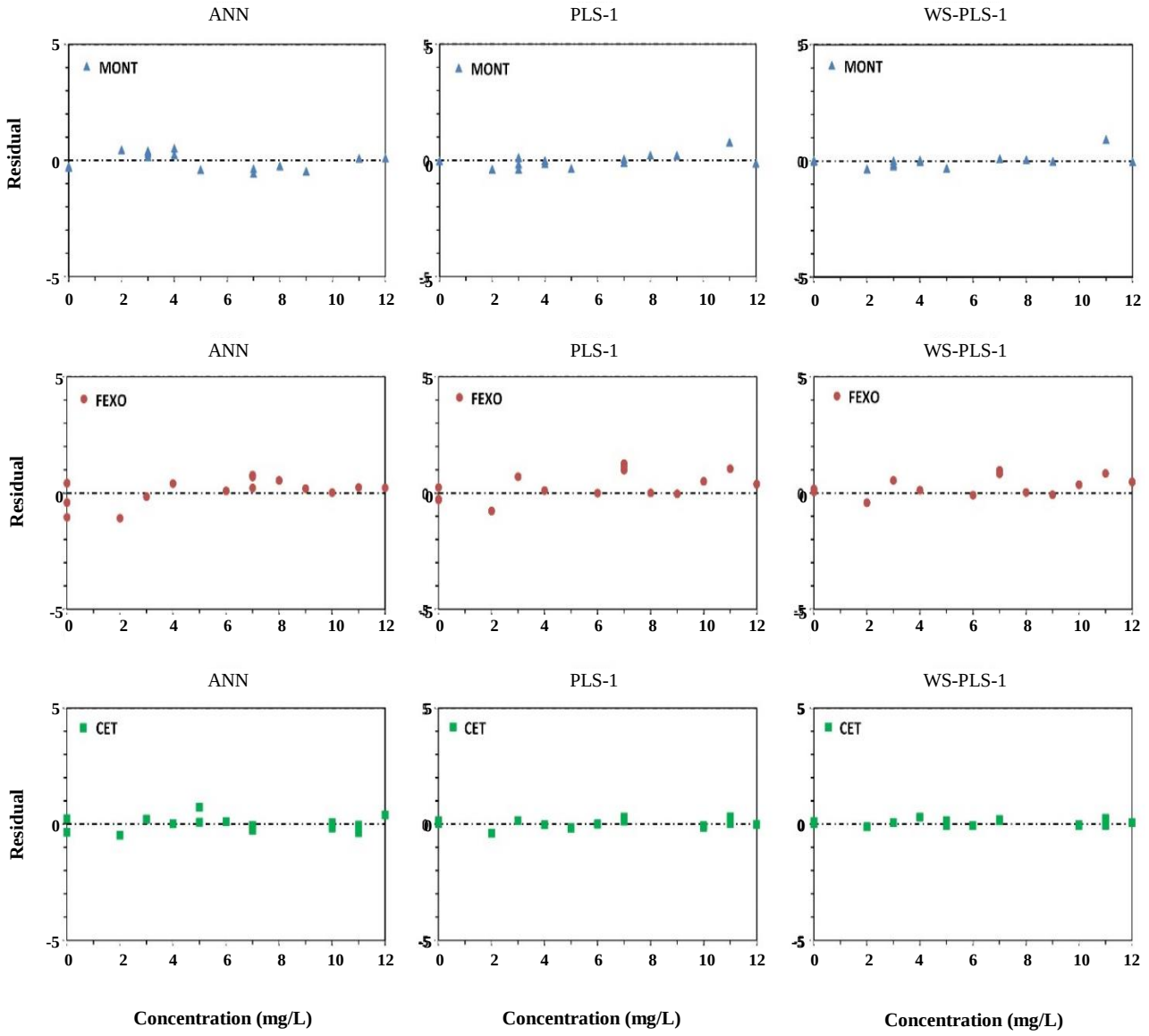

Fig. 9: Residual errors of different methods vs. concentration plots for the three components of test set.

it is understood that WS- PLS-1 method used less factors than PLS-1 and at the same time had a positive impact on the prediction accuracy for every component, however, this behavior was more pronounced in the case of FEXO. Based on the results, it can be deduced that WS-PLS-1 method has successfully quantified the amount of each compound in the studied pharmaceutical samples. Therefore, WS-PLS-1 method may be used as a powerful chemometric tool in drug analysis applications combined with UV-Vis spectroscopy.

CONCLUSIONS

The present work studied the simultaneous quantification of MONT, FEXO and CET with the aid of UV-Vis spectroscopy combined with different chemometric techniques. In order to identify the most suitable chemometric method, various calibration models including PLS-1, WS- PLS-1 and ANN were developed and validated by an independent test set of drug mixtures. The cross-validation leave-one-sample-out procedure was applied in the present work to obtain the optimum factors

Table 5: Statistical parameters and optimum number of factors for calibration and test sets by PLS-1, WS-PLS-1 and ANN regression for three drugs.

	MONT			FEXO			CET		
Parameters	PLS-1	WS-PLS-1	ANN	PLS-1	WS-PLS-1	ANN	PLS-1	WS-PLS-1	ANN
A[a]	3	3	2	5	3	4	8	3	3
RMSEP	0.284	0.277	0.353	0.670	0.511	0.540	0.179	0.138	0.303
R^2_{pred}	0.993	0.994	0.991	0.966	0.982	0.978	0.998	0.999	0.994
REP (%)	4.55	4.45	5.54	10.27	7.75	8.01	2.47	1.90	4.16

during calibration. Performance of ANN was also optimized through manipulating different network parameters and architectures. It was found that PLS-1 and ANN methods exhibited satisfactory performances. In addition, applying wavelength selection methodology for PLS-1 model have had a positive impact on prediction performance of PLS-1 model. Several figures of merit such as LOD and analytical sensitivity were calculated and their values were significantly enhanced by WS-PLS-1 rather than PLS-1 method. Specifically, LODs provided by WS-PLS-1 method were found to be 0.029, 0.049 and 0.054 mg L^{-1} for MONT, FEXO and CET, respectively. The results indicated that WS-PLS-1 is capable of capturing the interactions between components with highly-overlapped absorption spectra with a good degree of accuracy.

Received : Jun. 17, 2016 ; Accepted : Oct. 17, 2016

REFERENCES

[1] Ibrahim M.A., Amin E.F., Ibrahim S.A., Abdelzaher W.Y., Abdelrahman A.M., Montelukast and Irbesartan Ameliorate Metabolic and Hepatic Disorders in Fructose-Induced Metabolic Syndrome in Rats, *European Journal of Pharmacology*, **724**(0): 204-210 (2014).

[2] Simpson K., Jarvis B., Fexofenadine, *Drugs*, **59**(2):301-321 (2000).

[3] Samadi-Maybodi A., Nejad-Darzi S.K.H., Simultaneous Determination of Paracetamol, Phenylephrine Hydrochloride and Chlorpheniramine Maleate in Pharmaceutical Preparations Using Multivariate Calibration 1, *Spectrochimica Acta Part A: Molecular and Biomolecular Spectroscopy*, **75**(4):1270-1274 (2010).

[4] Ahmadi S.H., Tavakoli H., Amirzadeh M., Sangi M.R., Simultaneous Determination of Hydrochlorothiazide and Enalapril Maleate in Pharmaceutical Formulations Using Fourier Transform Infrared Spectrometry, *Iranian Journal of Chemistry and Chemical Engineering (IJCCE)*, **33**(4):59-68 (2014).

[5] Masoum S., Alishahi A. R., Farahmand H., Shekarchi M., Prieto N., Determination of Protein and Moisture in Fishmeal by Near-Infrared Reflectance Spectroscopy and Multivariate Regression Based on Partial Least Squares, *Iranian Journal of Chemistry and Chemical Engineering (IJCCE)*, **31**(3):51-59 (2012).

[6] Rouhollahi A., Tavakoli H., Nayebi S., Ghasemi J., Noroozi M., Hashemi M., Simultaneous Spectrophotometric Determination of Heavy Metal Ions Using Several Chemometrics Methods: Effect of Different Parameters of Savitzky-Golay and Direct Orthogonal Signal Correction Filters, *Iranian Journal of Chemistry and Chemical Engineering (IJCCE)*, **26**(2):41-51 (2007).

[7] Goicoechea H. C., Olivieri A. C., Enhanced Synchronous Spectrofluorometric Determination of Tetracycline in Blood Serum by Chemometric Analysis. Comparison of Partial Least-squares and Hybrid Linear Analysis Calibrations, *Analytical Chemistry*, **71**(19):4361-4368 (1999).

[8] Shariati-Rad M., Irandoust M., Amin N., and Ahmadi F., Simultaneous Determination of Paracetamol, Dextromethorphan, Phenylephrine and Chlorpheniramine Using Partial Least Squares, *Current Pharmaceutical Analysis*, **9**(2): 183-190 (2013).

[9] Martens H., Naes T., "Assessment, Validation and Choice of Calibration Method, Multivariate Calibration", Wiley: New York, 237-266 (1989).

[10] Khoshayand M. R., Abdollahi H., Shariatpanahi M., Saadatfard A., Mohammadi A., Simultaneous Spectrophotometric Determination of Paracetamol, Ibuprofen and Caffeine in Pharmaceuticals by Chemometric Methods, *Spectrochimica Acta Part A: Molecular and Biomolecular Spectroscopy*, **70**(3):491-499 (2008).

[11] Khanmohammadi M., Karimi M.A., Ghasemi K., Jabbari M., and Garmarudi A.B., Quantitative Determination of Malathion in Pesticide by Modified Attenuated Total Reflectance-Fourier Transform Infrared Spectrometry Applying Genetic Algorithm Wavelength Selection Method, *Talanta*, **72**(2): 620-625 (2007).

[12] Leardi R., Genetic Algorithms in Chemometrics and Chemistry: a Review, *Journal of Chemometrics*, **15**(7):559-569 (2001).

[13] Fatemi S., Masoori M., and Bozorgmehry Boozarjomehry R., Application of Genetic Algorithm in Kinetic Modeling and Reaction Mechanism Studies, *Iranian Journal of Chemistry and Chemical Engineering (IJCCE)*, **24**(4):37-46 (2005).

[14] Sadi M. and Dabir B., Application of Genetic Algorithm to Determine Kinetic Parameters of Free Radical Polymerization of Vinyl Acetate by Multi-Objective Optimization Technique, *Iranian Journal of Chemistry and Chemical Engineering (IJCCE)*, **26**(4): 29-37 (2007).

[15] Marsili N.R., Sobrero M.S., Goicoechea H.C., Spectrophotometric Determination of Sorbic and Benzoic Acids in Fruit Juices by a Net Analyte Signal-Based Method with Selection of the Wavelength Range to Avoid Non-Modelled Interferences, *Analytical and Bioanalytical Chemistry*, **376**(1):126-133 (2003).

[16] Mohagheghian E., Zafarian-Rigaki H., Motamedi-Ghahfarrokhi Y., Hemmati-Sarapardeh A., Using an Artificial Neural Network to Predict Carbon Dioxide Compressibility Factor at High Pressure and Temperature, *Korean Journal of Chemical Engineering*, 1-10 (2015).

[17] Ehsani M. R., Bateni H., Razi Parchikolaei G., Modeling of Oxidative Coupling of Methane over Mn/Na2WO4/SiO2 Catalyst Using Artificial Neural Network, *Iranian Journal of Chemistry and Chemical Engineering (IJCCE)*, **32**(3):107-114 (2013).

[18] Chamsaz M., Safavi A., Fadaee J., Simultaneous Kinetic-Spectrophotometric Determination of Carbidopa, Levodopa and Methyldopa in the Presence of Citrate with the Aid of Multivariate Calibration and Artificial Neural Networks, *Analytica Chimica Acta*, **603**(2):140-146 (2007).

[19] Khoshayand M. R., Abdollahi H., Shariatpanahi M., Saadatfard A., Mohammadi A., Simultaneous Spectrophotometric Determination of Paracetamol, Ibuprofen and Caffeine in Pharmaceuticals by Chemometric Methods, *Spectrochimica Acta Part A: Molecular and Biomolecular Spectroscopy*, **70**(3):491-499 (2008).

[20] Li B., He Y., Xu C., Simultaneous Determination of Three Organophosphorus Pesticides Residues in Vegetables Using Continuous-Flow Chemiluminescence with Artificial Neural Network Calibration, *Talanta*, **72**(1):223-230 (2007).

[21] Ni Y., Huang C., Kokot S., Application of Multivariate Calibration and Artificial Neural Networks to Simultaneous Kinetic-Spectrophotometric Determination of Carbamate Pesticides, *Chemometrics and Intelligent Laboratory Systems*, **71**(2):177-193 (2004).

[22] Li Q., Yao X., Chen X., Liu M., Zhang R., Zhang X., Hu Z., Application of Artificial Neural Networks for the Simultaneous Determination of a Mixture of Fluorescent Dyes by Synchronous Fluorescence, *Analyst*, **125**(11):2049-2053 (2000).

[23] Olivieri A. C., Goicoechea H. C., Iñón F. A., MVC1: An Integrated MatLab Toolbox for First-Order Multivariate Calibration, *Chemometrics and Intelligent Laboratory Systems*, **73**(2):189-197 (2004).

[24] Gholivand M. B., Shariati-Rad M., Karimian N., Torkashvand M., A Chemometrics Approach for Simultaneous Determination of Cyanazine and Propazine Based on a Carbon Paste Electrode Modified by a Molecularly Imprinted Polymer, *Analyst*, **137**(5):1190-1198 (2012).

[25] Shariati- Rad M., Hasani M., Selection of Individual Variables Versus Intervals of Variables in PLSR, *Journal of Chemometrics*, **24**(2):45-56 (2010).

[26] Shariati-Rad M., Irandoust M., Amin N., Shamsipur M., Solving Matrix Effect, Spectral Interferences and Nonlinearity by Generalized Standard Addition Method Coupled with Radial Basis Functions-Partial Least Squares: Application to Simultaneous Determination of Drugs in Urine, *Chemometrics and Intelligent Laboratory Systems*, **120**(77-83 (2013).

[27] Tarjomannejad A., Prediction of the Liquid Vapor Pressure Using the Artificial Neural Network-Group Contribution Method, *Iranian Journal of Chemistry and Chemical Engineering (IJCCE)*, **34**(4):97-111 (2015).

[28] Tymvios F. S., Michaelides S. C., Skouteli C. S., "Estimation of Surface Solar Radiation with Artificial Neural Networks. In Modeling Solar Radiation at the Earth's Surface" Springer Berlin Heidelberg (2008).

[29] Thomas E. V., Haaland D. M., Comparison of Multivariate Calibration Methods for Quantitative Spectral Analysis, *Analytical Chemistry*, **62**(10):1091-1099 (1990).

[30] Ragno G., Ioele G., Risoli A., Multivariate Calibration Techniques Applied to the Spectrophotometric Analysis of one-to-four Component Systems, *Analytica Chimica Acta*, **512**(1):173-180 (2004).

[31] Marsili N. R., Sobrero M. S., Goicoechea H. C., Spectrophotometric Determination of Sorbic and Benzoic Acids in Fruit Juices by a Net Analyte Signal-Based Method with Selection of the Wavelength Range to Avoid Non-Modelled Interferences, *Analytical and Bioanalytical Chemistry*, **376**(1):126-133 (2003).

[32] Lorber A., Faber K., Kowalski B. R., Net Analyte Signal Calculation in Multivariate Calibration, *Analytical Chemistry*, **69**(8):1620-1626 (1997).

[33] Booksh K. S., Kowalski B. R., Theory of Analytical Chemistry, *Analytical Chemistry*, **66**(15):782A-791A (1994).

[34] Goicoechea H. C., Olivieri A. C., Determination of Bromhexine in Cough–Cold Syrups by Absorption Spectrophotometry and Multivariate Calibration Using Partial Least-Squares and Hybrid Linear Analyses. Application of a Novel Method of Wavelength Selection, *Talanta*, **49**(4):793-800 (1999).

[35] C. Goicoechea H., C. Goicoechea H., C. Olivieri A., Wavelength Selection by Net Analyte Signals Calculated with Multivariate Factor-Based Hybrid Linear Analysis (HLA). A Theoretical and Experimental Comparison with Partial Least-Squares (PLS), *Analyst*, **124**(5):725-731 (1999).

[36] Skibsted E.T.S., Boelens H.F.M., Westerhuis J.A., Witte D.T., Smilde A.K., New Indicator for Optimal Preprocessing and Wavelength Selection of Near-Infrared Spectra, *Applied Spectroscopy*, **58**(3): 264-271 (2004).

[37] Vekaria H., Limbasiya V., Patel P., Development and Validation of RP-HPLC Method for Simultaneous Estimation of Montelukast Sodium and Fexofenadine Hydrochloride in Combined Dosage Form, *Journal of Pharmacy Research*, **6**(1):134-139 (2013).

[38] Roman J., Breier A. R., Steppe M., Stability Indicating LC Method to Determination of Sodium Montelukast in Pharmaceutical Dosage form and Its Photodegradation Kinetics, *Journal of Chromatographic Science*, **49**(7):540-546 (2011).

[39] Alsarra I., Al-Omar M., Gadkariem E., Belal F., Voltammetric Determination of Montelukast Sodium in Dosage Forms and Human Plasma, *Il Farmaco*, **60**(6):563-567 (2005).

[40] Yıldız G., Aydoğmuş Z., Kauffmann J. M., Differential Pulse Voltammetric Determination of Montelukast in Tablets and Human Plasma by Using Chitosan Modified Carbon Paste Electrode, *Electroanalysis*, **25**(7):1796-1802 (2013).

[41] Arayne M. S., Sultana N., Hussain F., Spectrophotometric Method for Quantitative Determination of Montelukast in Bulk, Pharmaceutical Formulations and Human Serum, *Journal of Analytical Chemistry*, **64**(7):690-695 (2009).

[42] Radhakrishna T., Reddy G. O., Simultaneous Determination of Fexofenadine and Its Related Compounds by HPLC, *Journal of Pharmaceutical and Biomedical Analysis*, **29**(4):681-690 (2002).

[43] Zafar F., Shoaib M. H., Yousuf R. I., Development of RP-HPLC Method for Fexofenadine Determination in Tablet Formulations and Development of Dissolution Method, *Pakistan Journal of Pharmacology*, **28**:43-49 (2011).

[44] El-Hay S. S. A., Colyer C. L., Hassan W. S., Shalaby A., Spectrofluorimetric Determination of Etodolac, Moxepril HCl and Fexofenadine HCl Using Europium Sensitized Fluorescence in Bulk and Pharmaceutical Preparations, *Journal of Fluorescence*, **22**(1):247-252 (2012).

[45] Karakuş S., Küçükgüzel İ., Küçükgüzel Ş. G., Development and Validation of a Rapid RP-HPLC Method for the Determination of Cetirizine or Fexofenadine with Pseudoephedrine in Binary Pharmaceutical Dosage Forms, *Journal of Pharmaceutical and Biomedical Analysis*, **46**(2):295-302 (2008).

[46] El Walily A., Korany M., El Gindy A., Bedair M., Spectrophotometric and high Performance Liquid Chromatographic Determination of Cetirizine Dihydrochloride in Pharmaceutical Tablets, *Journal of Pharmaceutical and Biomedical Analysis*, **17**(3):435-442 (1998).

[47] Javid F. S., Shafaat A., Zarghi A., Determination of Cetirizine and Its Impurities in Bulk and Tablet Formulation Using a Validated Capillary Zone Electrophoretic Method, *Journal of Analytical Chemistry*, **69**(5):442-447 (2014).

[48] Ahmed S., Atia N. N., Simultaneous Determination of Montelukast as Sparing Therapy with Some Inhaled Corticosteroids in Plasma of Asthmatic Patients, *Journal of Pharmaceutical and Biomedical Analysis*, **74**(250-256 (2013).

[49] Kitchen C.J., Wang A.Q., Musson D.G., Yang A.Y., Fisher A.L., A Semi-Automated 96-Well Protein Precipitation Method for the Determination of Montelukast in Human Plasma Using High Performance Liquid Chromatography/Fluorescence Detection, *Journal of Pharmaceutical and Biomedical Analysis*, **31**(4):647-654 (2003).

[50] Ranjan O.P., Nayak U.Y., Reddy M.S., Dengale S.J., Musmade P.B., Udupa N., Development and Validation of RP-HPLC Method with Ultraviolet Detection for Estimation of Montelukast in Rabbit Plasma: Application to Preclinical Pharmacokinetics, *Journal of Young Pharmacists*, **5**(4):133-138 (2013).

[51] Heli H., Sattarahmady N., Vais R. D., Karimian K., Nickel Hydroxide Nanopetals: One-pot Green Synthesis, Characterization and Application for the Electrocatalytic Oxidation and Sensitive Detection of Montelukast, *Sensors and Actuators B: Chemical*, **196**:631-639 (2014).

[52] Arayne M. S., Sultana N., Shehnaz H., Haider A., RP-HPLC Method for the Quantitative Determination of Fexofenadine Hydrochloride in Coated Tablets and Human Serum, *Medicinal Chemistry Research*, **20**(1):55-61 (2011).

[53] Miura M., Uno T., Tateishi T., Suzuki T., Determination of Fexofenadine Enantiomers in Human Plasma with High-Performance Liquid Chromatography, *Journal of Pharmaceutical and Biomedical Analysis*, **43**(2):741-745 (2007).

[54] Uno T., Yasui-Furukori N., Takahata T., Sugawara K., Tateishi T., Liquid Chromatographic Determination of Fexofenadine in Human Plasma with Fluorescence Detection, *Journal of Pharmaceutical and Biomedical Analysis*, **35**(4):937-942 (2004).

[55] Alothman Z.A., Bukhari N., Haider S., Wabaidur S.M., Alwarthan A. A., Spectrofluorimetric Determination of Fexofenadine Hydrochloride in Pharmaceutical Preparation Using Silver Nanoparticles, *Arabian Journal of Chemistry*, **3**(4):251-255 (2010).

[56] Hadad G.M., Emara S., Mahmoud W.M., Development and Validation of a Stability-Indicating RP-HPLC Method for the Determination of Paracetamol with Dantrolene or/and Cetirizine and Pseudoephedrine in Two Pharmaceutical Dosage Forms, *Talanta*, **79**(5):1360-1367 (2009).

[57] Jaber A., Al Sherife H., Al Omari M., Badwan A., Determination of Cetirizine Dihydrochloride, Related Impurities and Preservatives in Oral Solution and Tablet Dosage Forms Using HPLC, *Journal of Pharmaceutical and Biomedical Analysis*, **36**(2):341-350 (2004).

[58] Rosseel M., Lefebvre R., Determination of Cetirizine in Human Urine by High-Performance Liquid Chromatography, *Journal of Chromatography B: Biomedical Sciences and Applications*, **565**(1):504-510 (1991).

[59] Ma M., Feng F., Sheng Y., Cui S., Liu H., Development and Evaluation of an Efficient HPLC/MS/MS Method for the Simultaneous Determination of Pseudoephedrine and Cetirizine in Human Plasma: Application to Phase-I Pharmacokinetic Study, *Journal of Chromatography B*, **846**(1):105-111 (2007).

[60] Patil R.H., Hegde R.N., Nandibewoor S. T., Electro-Oxidation and Determination of Antihistamine Drug, Cetirizine Dihydrochloride at Glassy Carbon Electrode Modified with Multi-Walled Carbon Nanotubes, *Colloids and Surfaces B: Biointerfaces*, **83**(1):133-138 (2011).